Heliyon 10 (2024) e23526

Contents lists available at ScienceDirect

Heliyon

journal homepage: www.cell.com/heliyon

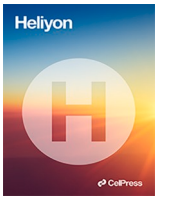

CYP2J2-derived epoxyeicosatrienoic acids protect against doxorubicin-induced cardiotoxicity by reducing oxidative stress and apoptosis via activation of the AMPK pathway

Chuanmeng Zhu [a], Yang Bai [a], Jie Qiu [a], Guangzhi Chen [a], Xiaomei Guo [a,**], Renfan Xu [b,*]

[a] *Division of Cardiology, Department of Internal Medicine, Tongji Hospital, Tongji Medical College, Huazhong University of Science and Technology, Wuhan, 430030, China*

[b] *Department of Medical Ultrasound, Tongji Hospital, Tongji Medical College, Huazhong University of Science and Technology, Wuhan, 430030, China*

ARTICLE INFO

Keywords:
Cardiotoxicity
Doxorubicin
EETs
Apoptosis
Oxidative stress
AMPK

ABSTRACT

Objective: Despite the widespread use of doxorubicin (DOX) in chemotherapy, it can cause cardiotoxicity, which severely limits its potential clinical use. CYP2J2-derived epoxyeicosatrienoic acids (EETs) exert cardioprotective effects by maintaining cardiac homeostasis. The roles and latent mechanisms of EETs in DOX cardiotoxicity remain uncertain. We investigated these aspects using mouse tissue and cell culture models.

Methods: C57BL/6J mice were injected with rAAV9-CYP2J2 or a control vector via the caudal vein. A five-week intraperitoneal course of DOX (5 mg/kg per week) was administered. After pretreatment with 14,15-EET, H9C2 cells were treated for 24-h with DOX, to use as a cell model to verify the role of EETs in cardiotoxicity *in vitro*.

Results: CYP2J2 overexpression mitigated DOX-induced cardiotoxicity, as shown by the diminished cardiac injury marker levels, improved heart function, reduced oxidative stress, and inhibition of myocardial apoptosis *in vivo*. These protective roles are associated with the enhancement of antioxidant and anti-apoptotic abilities and the activation of the AMPK pathway. 14,15-EET suppresses DOX-induced oxidative stress, mitochondrial dysfunction, and apoptosis in H9C2 cells. AMPK knockdown partially abolished the cardioprotective effects of 14,15-EET against oxidative damage and apoptosis in DOX-treated cells, suggesting that AMPK is responsible for EET-mediated protection against cardiotoxicity.

Conclusion: CYP2J2-derived EETs confer myocardial protection against DOX-induced toxicity by activating the AMPK pathway, which reduces oxidative stress, mitochondrial dysfunction, and apoptosis.

* Corresponding author. Department of Medical Ultrasound, Tongji Hospital, Tongji Medical College, Huazhong University of Science and Technology, 1095# Jiefang Ave., 430030, Wuhan, China.

** Corresponding author. Division of Cardiology, Department of Internal Medicine, Tongji Hospital, Tongji Medical College, Huazhong University of Science and Technology, 1095# Jiefang Ave., 430030, Wuhan, China.

E-mail addresses: xmguo@hust.edu.cn (X. Guo), xurenfantjh@163.com (R. Xu).

https://doi.org/10.1016/j.heliyon.2023.e23526
Received 18 June 2023; Received in revised form 5 December 2023; Accepted 5 December 2023
Available online 9 December 2023

1. Introduction

The chemotherapeutic agent doxorubicin (DOX), an anthracycline, is commonly used to treat a variety of malignant tumors such as sarcomas, carcinomas, and hematological malignancies [1]. Due to its progressive cardiovascular side effects during chemotherapy, DOX is restricted in clinical use as it may lead to heart failure [2,3].

DOX cardiotoxicity is mediated by oxidative stress, autophagy disorder, mitochondrial dysfunction, and apoptosis [3,4]. Reactive oxygen species (ROS) and cardiomyocyte apoptosis are considered as the major contributors to DOX-induced myocardial damage and dysfunction [2]. ROS not only causes oxidative damage to biomolecules but also disrupts cell membrane integrity and function, and excess free radicals trigger intrinsic mitochondrial-dependent apoptotic pathways, leading to cardiomyocyte death [5,6]. DOX-induced injury, myocardial apoptosis, and caspase activation play key roles in the progression of congestive heart failure. Excess free radicals trigger the intrinsic mitochondria-dependent apoptotic pathway, that causes cardiomyocyte death [7]. Therefore, the inhibition of oxidative stress and apoptosis are beneficial for the improvement of DOX-related cardiac damage and dysfunction, as confirmed by many recent studies [8,9].

One of the main arachidonic acid cycde-synthases, CYP2J2 is abundantly expressed in coronary artery endothelial cells, cardiomyocytes, and smooth muscle cells. Accumulating evidence indicates that CYP2J2 and its epoxyeicosatrienoic acid (EET) products have multiple cardioprotective effects, including amelioration of inflammatory reactions, inhibition of apoptosis, and reduction of cardiac remodeling and hypertrophy [10]. Previous studies have demonstrated that overexpression of cardiomyocyte-specific CYP2J2 can reduce oxidative stress-mediated endoplasmic reticulum stress and NF-κB p65 nuclear translocation to inhibit angiotensin II-mediated cardiac remodeling, dysfunction, and heart failure [11]. Few studies have explored the cardioprotective effects of CYP2J2 or the potential impact of arachidonic acid products on DOX-mediated toxicity.

Adenosine monophosphate-activated protein kinase (AMPK), is a pivotal central regulator and sensor in maintaining homeostasis in the energy system. Previous studies indicated that DOX treatment suppresses AMPK protein and phosphorylation levels [12]. Further studies have confirmed that AMPK activation alleviates acute DOX cardiotoxicity by reducing cardiac injury, oxidative stress, mitochondrial dysfunction, and myocardial apoptosis [13]. Therefore, targeting AMPK may have notable therapeutic implications in DOX-mediated cardiotoxicity. In this context, 14,15-EET is reported to activate the AMPK signaling pathway [14]. Based on this view, targeting AMPK may have significant therapeutic implications for DOX-mediated cardiotoxicity. Currently, the roles and underlying mechanisms of EETs in DOX cardiotoxicity remain largely unknown. We hypothesized that the overexpression of CYP2J2 may protect heart from DOX exposure. Thus, our study aimed to explore the mechanisms underlying the cardioprotective effects of CYP2J2 and to investigate whether AMPK plays a pivotal role in this process.

2. Materials and methods

2.1. Animal experiment

Eight-week-old male C57BL/6J mice were purchased from GemPharmatech (Nanjing, China). The protocols for animal experiments were approved by the Institutional Animal Research Committee (NO:TJH-20201006) of Tongji Hospital, Tongji Medical College (Wuhan, China) and conducted in accordance with the ARRIVE and NIH guidelines. Recombinant adeno-associated viruses (rAAV) expressing green fluorescent protein (GFP) or CYP2J2 were generated via triple plasmid co-transfection into HEK293 cells [15,16]. The mice were kept in a pathogen-free environment at normal atmospheric temperature (22 °C ± 2 °C) with an adequate diet and fresh water, free of charge. After acclimatization for 7 d, four groups of mice were selected and randomly divided as follows: 1) rAAV9-GFP, 2) rAAV9-CYP2J2, 3) DOX + rAAV9-GFP, and 4) DOX + rAAV9-CYP2J2 (n = 10 per group). Purified vectors of rAAV9-CYP2J2 (1×10^{11} pfu) or rAAV9-GFP (1×10^{11} pfu) were administered via the caudal vein [17]. Two weeks after rAAV9 injection, the mice were intraperitoneally injected with DOX (5 mg/kg/week) or the same volume of saline solution for five weeks [18]. All mice were weighed weekly and euthanized on seven days after the final dose of DOX. After echocardiographic assessment, blood samples were obtained and serum was collected for further experiments. After harvesting, the heart tissue was cut in half, and parts of the heart were stored in 10 % neutral-buffered formalin. The remaining heart tissue was frozen at −80 °C for further biochemical analysis.

2.2. Echocardiographic and hemodynamic measurements

In accordance with previous studies, echocardiographic measurements were performed using a high-frequency (30 MHz) ultrasound probe designed for small animals (Vevo 1100, Visual Sonics, Toronto, Canada) [19]. We measured the hemodynamics of the left ventricle using a Millar catheter system [20].

2.3. Histological assays

Slices (4 mm) were cut from the formalin-fixed hearts embedded in paraffin. The sections were subjected to hematoxylin and eosin (HE) and Masson's trichrome staining. To assess ROS production, fresh frozen heart tissues were embedded in optimal cutting temperature compound (Tissue-Tek, Sakura Finetech, Torrance, CA, USA) and sliced to 5 μm.

2.4. Enzyme-linked immunosorbent assay

According to the manufacturer's instructions, ELISA kits (Jiancheng, Nanjing, China) were used to analyze serum cardiac injury markers, including cTnT, CK-MB, and LDH.

2.5. Cell culture and treatment

The H9C2 cell line was purchased from the American Type Culture Collection (ATCC, Manassas, VA, USA). H9C2 cells were cultured in Dulbecco's modified Eagle's medium containing 10 % fetal bovine serum, 4 mL glutamine, and 100 U/mL penicillin–streptomycin in 75 cm^2 tissue culture flasks. Cells were grown in 95 % relative humidity under 37 °C humidity and 5 % CO2. To explore the roles of 14,15-EET in DOX-induced myocardial injury, H9C2 cells (1×10^4 cells/ml) were cultured with 1 μM DOX for 24 h after pretreatment with 1 μM 14,15-EET or 14,15-EEZE for 60 min (Supplementary Table S3).

2.6. Cell transfection and treatment

Transfection of small interfering RNAs (siRNA) was performed on the cells (1×10^4 cells/ml), including si-con or si-AMPKα (Guangzhou Ruibo Biotechnology, Guangzhou, China). After 24 h of transfection, the cells were cultured with DOX (1 μM) for 24 h in the presence or absence of 14,15-EET (1 μM). siRNA knockdown efficiency was evaluated by western blotting 48 h after transfection. Only silent effects greater than 70 % were considered in the experiments. All procedures were performed according to manufacturer's instructions.

2.7. Flow cytometry analysis

Apoptosis of H9C2 cells in each group was detected using an Annexin V/PI Apoptosis Detection Kit (KTA0004; Abbkine, Wuhan, China). The manufacturer's instructions were followed for all operations. Quantitative analyses were performed using the CytoFLEX flow cytometer (Beckman Coulter, Brea, California, USA).

2.8. Oxidative stress level and mitochondrial function detection

ROS generation in the cardiac tissue and H9C2 cells were detected using dihydroethidium (DHE) and 2′,7′-dichloro-dihydrofluorescein diacetate (DCFH-DA) staining respectively through commercially available kits (Keygen Biotech; Abbkine). A saturated phosphate buffer saline solution was used to wash the sections after incubation with DHE or DCFH-DA for 30 min at 37 °C in the dark. The fluorescence was detected using a fluorescence microscope (IX53; Olympus). The mean fluorescence intensity was calculated using ImageJ software (NIH, Bethesda, MA, USA). To further assess oxidative stress levels: MDA and GSH contents and SOD activity in cardiac tissues and cells were detected using commercially available kits (Jiancheng, Nanjing, China). Follow the instructions of mitochondrial membrane potential assay kit with JC-1 (Beyotime), fluorescence microscope to detect the fluorescence of JC-1 aggregates (red) and monomers (green) in cells.

2.9. RNA extraction and quantitative reverse transcription-polymerase chain reaction (qRT-PCR)

RNA was extracted from the heart tissue or cardiomyocytes using TRIzol reagent (Invitrogen, Waltham, MA, USA). Further, the enriched mRNA was reverse transcribed to complementary DNA (cDNA) using random primers and the HiScript® 1st Strand cDNA Synthesis Kit (Vazyme Biotech, Nanjing, China). qRT-PCR analysis was performed using a SYBR Rapid Quantitative PCR Kit (Vazyme Biotech, Nanjing, China) following the manufacturer's protocol. Primers used are listed in Supplementary Table S1.

2.10. Western blot

Cardiac tissues and cell samples were harvested and lysed using the RIPA solution. SDS-PAGE gels containing 12 % SDS were used to separate equal amounts of protein. The resolved proteins were transferred onto PVDF membranes by gel electrophoresis in transfer buffer consisting of 192 mM glycine, 20 % (v/v) methanol, and 0.02 % SDS. After blocking with 5 % non-fat milk in TBST at 25 °C for 1 h, the membranes were immunoblotted with the primary antibody overnight at 4 °C. Table S2 lists all primary antibodies. Membranes were then incubated with secondary antibodies at room temperature for 2 h. We quantified the intensity of the bands on the immunoblots detected by enhanced chemiluminescence using the ImageJ software.

2.11. Statistics

All data are presented as mean ± standard error of mean. Data were analyzed using a paired two-tailed *t*-test or one-way ANOVA, followed by Tukey's post-hoc test. GraphPad Prism 5 software (GraphPad Software, San Diego, CA, United States) was used for all analyses. Statistical significance was set at $p < 0.05$.

3. Results

3.1. Overexpression of CYP2J2 protected against cardiac dysfunction in mice treated with doxorubicin

CYP2J2 overexpression reduced the mortality rate of DOX-induced cardiotoxicity in mice (Fig. S1A). Western blotting demonstrated that there was no CYP2J2 protein expression in the hearts of WT or GFP treatment mice, however, abundant CYP2J2 protein expression was identified in mouse hearts after CYP2J2 treatment (Fig. S1B). There were no differences in body weights between the groups before DOX treatment. Two weeks after the first DOX injection, body weight was observed to be significantly reduced in the DOX group, whereas CYP2J2 overexpression attenuated the DOX-induced body weight loss (Fig. 1A). In the DOX group, the HW/TL ratio decreased significantly compared with that in the control group, which was prevented by CYP2J2 treatment (Fig. 1B).

Cardiac function parameters were measured using echocardiography and the Millar catheter system. Both LVEF and LVFS significantly reduced after DOX treatment. However, when accompanied by CYP2J2 overexpression, the decline in these parameters was less significant than that in the DOX group (Fig. 1C and D). Compared to the control group, the maximal rates of increase in left ventricular pressure (+dP/dt) and reduction in left ventricular pressure (-dP/dt) were significantly reversed in the DOX group (Fig. 1E–G). CYP2J2 treatment did not significantly affect cardiac function under basic conditions. CYP2J2 overexpression considerably reduced ANP and BNP mRNA levels in DOX-treated hearts (Fig. 1H and I). These data demonstrated that CYP2J2 overexpression protects against DOX-induced cardiac damage and dysfunction.

3.2. Overexpression of CYP2J2 alleviated cardiac atrophy and activated the AMPK pathway in DOX-treated mice

We performed HE and Masson's trichrome staining to evaluate myocyte size and fibrosis. Contrary to the control group, increased cardiac atrophy characterized by reduced cell size and increased fibrosis, was observed in the DOX group. CYP2J2 overexpression

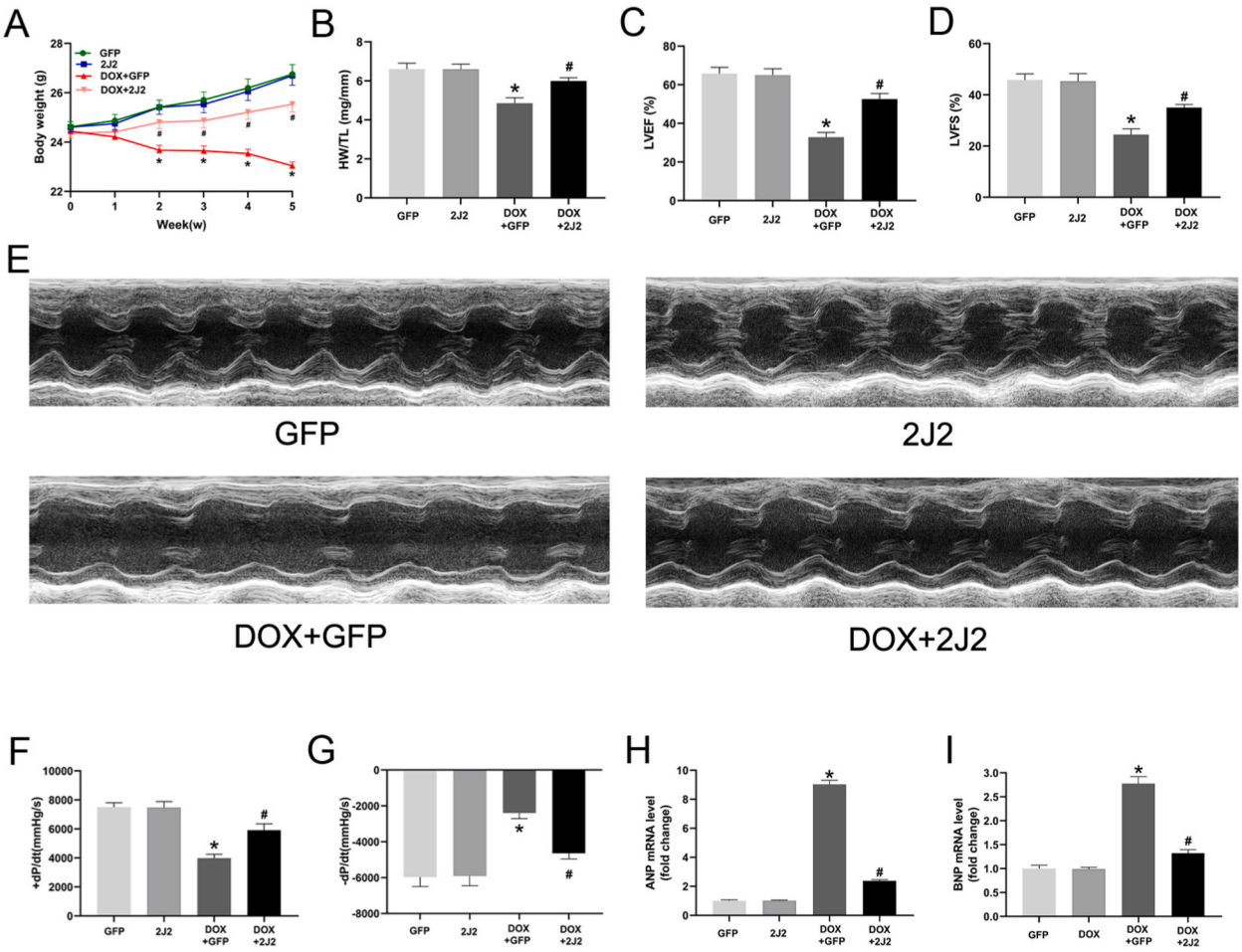

Fig. 1. Overexpression of CYP2J2 protected against cardiac dysfunction in DOX-treated mice. (A, B) Body weight and HW/TL ratio of mice in each group. (C–G) Representative echocardiographic and hemodynamic analyses in mice. (H, I) Relative cardiac mRNA levels of ANP and BNP in mice. Data are presented as the mean ± SEM (n = 7 per group). *$P < 0.05$ vs. GFP; #$P < 0.05$ vs. DOX + GFP.

significantly alleviated cardiac atrophy, as evidenced by larger cell sizes and smaller fibrotic areas compared to those in the DOX group (Fig. 2A, B, S1C, S1D). Moreover, a significant increase in cTnT, CK-MB, and LDH levels in the circulation was also observed following DOX exposure. CYP2J2 overexpression reduced these elevated levels (Fig. 2C–E).

To test whether the AMPK and PGC-1α signaling pathways were involved in CYP2J2-mediated cardiac protection *in vivo*, *p*-AMPKα, AMPKα, PGC-1α, and UCP2 levels were assessed by Western blot. A significant increase in *p*-AMPKα, PGC1α, and UCP2 levels was obtained in the CYP2J2 overexpression-treated mice exposed to DOX (Fig. 2F). These results suggest that CYP2J2 exerts cardioprotective effects against DOX-induced cardiac atrophy by activating AMPK.

3.3. Overexpression of CYP2J2 decreased cardiac oxidative stress, mitochondrial dysfunction and apoptosis in DOX-treated mice

Dihydroethidium (DHE) staining was performed to determine whether CYP2J2 overexpression inhibited DOX-induced oxidative damage. It was used to detect ROS levels, which showed inconspicuous red fluorescence in normal hearts. ROS levels significantly increased after DOX treatment, although not as significantly as in DOX-treated mice overexpressing CYP2J2 (Fig. 3A, S4A). The antioxidant capacity of CYP2J2 was further characterized using key enzymes such as GSH and SOD, which scavenge oxygen free radicals, as well as the oxidative stress index MDA. CYP2J2 overexpression significantly reduced the MDA content and enhanced the GSH levels and SOD activity in DOX-treated hearts (Fig. 3B). NOX2 and NOX4 are important subtypes of NADPH oxidases that are major sources of ROS in cardiomyocytes. Western blotting revealed that NOX2 and NOX4 levels were increased, whereas SOD1 and

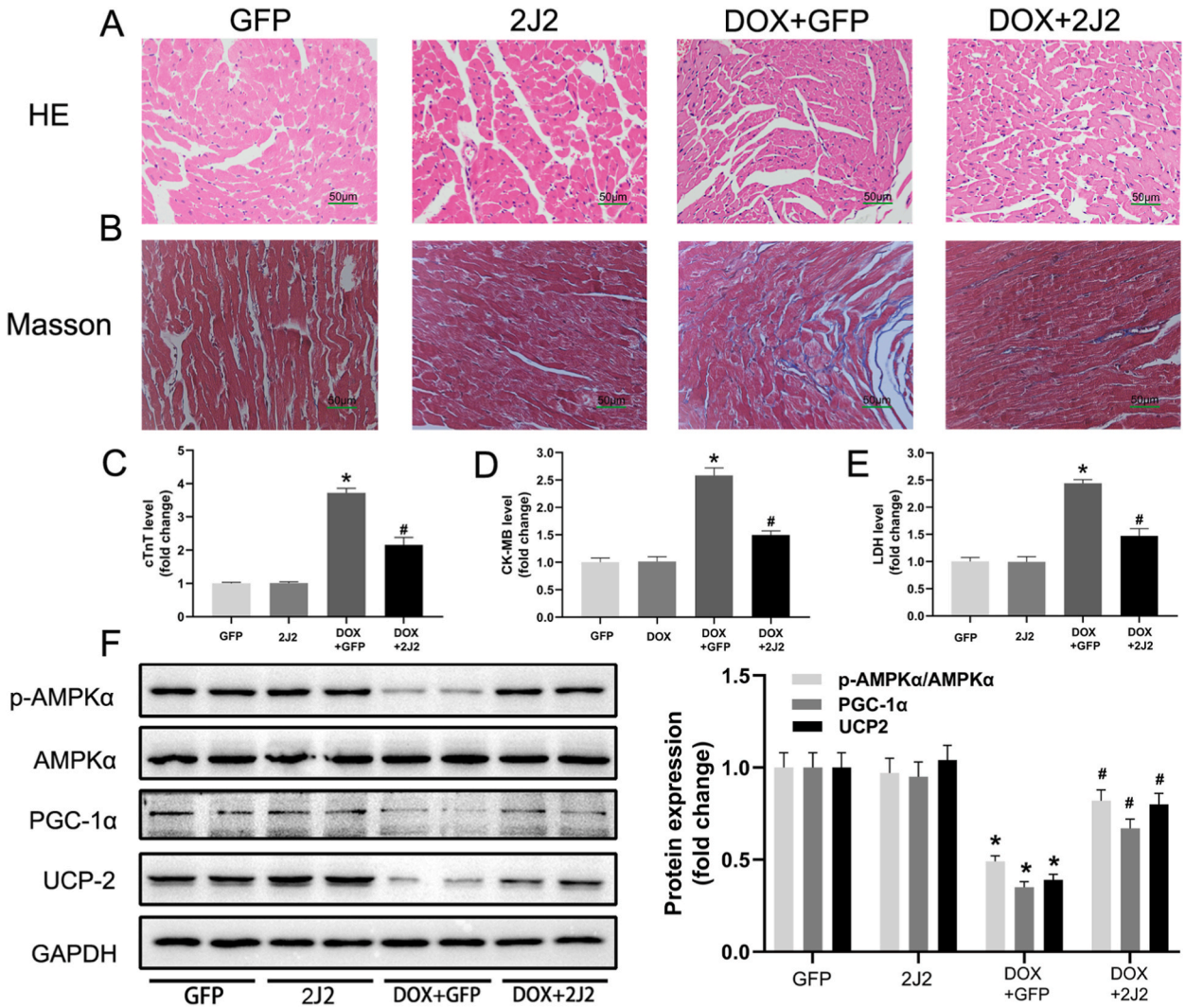

Fig. 2. Overexpression of CYP2J2 alleviated cardiac atrophy and activated AMPK pathway in DOX-treated mice. (A, B) HE and Masson's trichrome staining of heart sections from mice. (C–E) Serum levels of cTnT, CK-MB, LDH in mice were determined. (F) Representative immunoblots and quantitative analysis of *p*-AMPKα, AMPKα, PGC-1α, and UCP2 in the hearts from different groups. Data are presented as the mean ± SEM (n = 7 per group). $^{*}P < 0.05$ vs. GFP; $^{\#}P < 0.05$ vs. DOX + GFP.

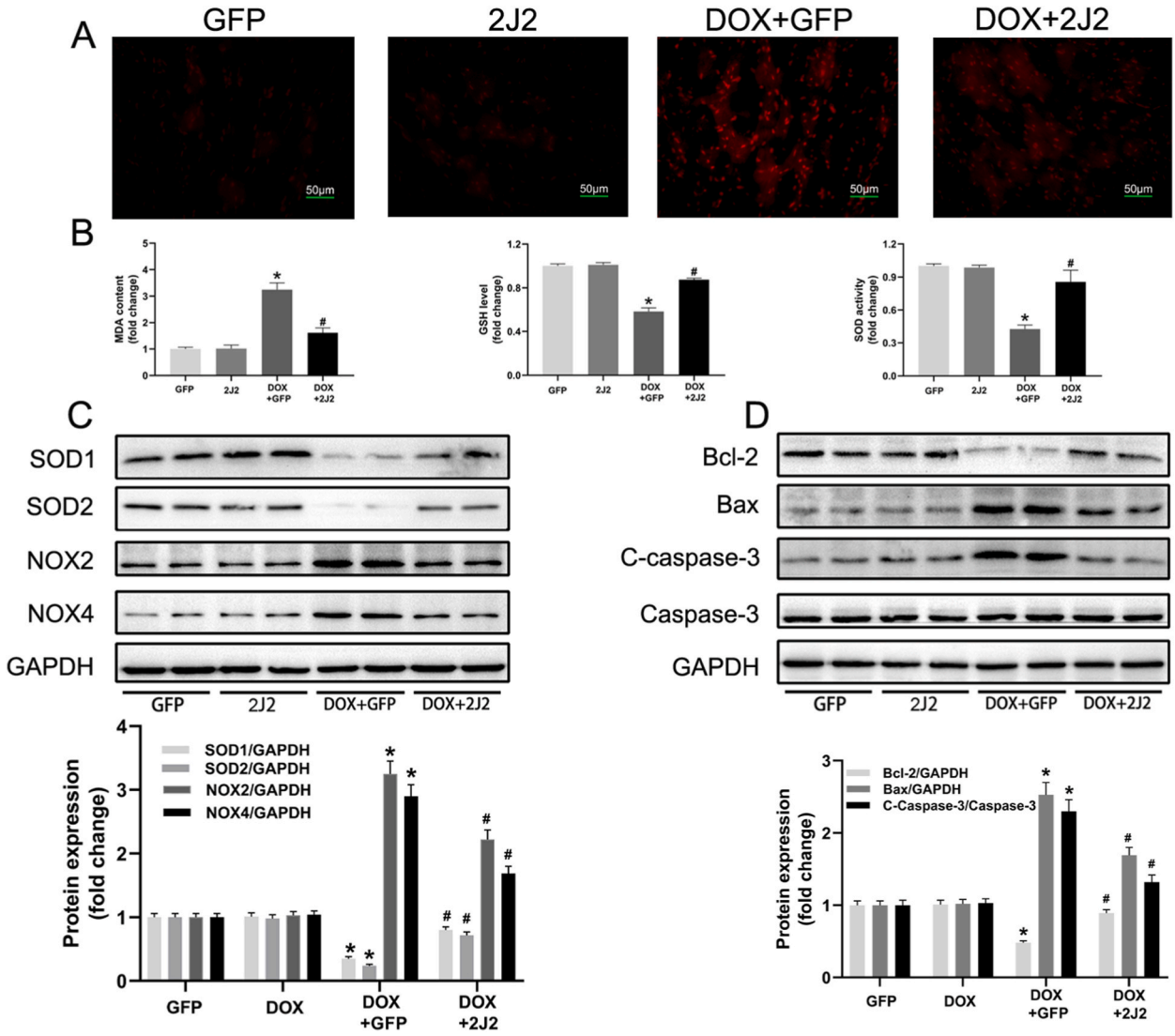

Fig. 3. Overexpression of CYP2J2 decreased cardiac oxidative stress, mitochondrial dysfunction, and apoptosis in DOX-treated mice. (A) Representative images of DHE staining of cardiac ROS production. (B) MDA content, GSH level, and SOD enzyme activity in the heart. (C) Representative immunoblots and quantitative analysis of SOD1, SOD2, NOX2 and NOX4 levels in the heart from different groups. (D) Representative immunoblots and quantitative analysis of Bcl-2, Bax, C-caspase-3, and caspase-3 levels in the heart from different groups. Data are presented as the mean ± SEM (n = 7 per group). $^{*}P < 0.05$ vs. GFP; $^{\#}P < 0.05$ vs. DOX + GFP.

SOD2 levels were significantly reduced in DOX-treated mice compared to control mice. CYP2J2 treatment dramatically reversed these changes (Fig. 3C), indicating that CYP2J2 overexpression alleviated excessive oxidative stress by increasing antioxidant enzyme levels and diminishing the oxidation products in DOX-treated mouse hearts.

Increased expression of DRP1, a key protein that controls mitochondrial fission in mammalian cells, promotes mitochondrial fission. Western blotting revealed that CYP2J2 overexpression prevented the upregulation of DRP1, which is a mitochondrial fission marker (Fig. S2A). Cytochrome C is one of the mitochondrial proteins that is released into the cytosol when the cell is activated by an apoptotic stimulus. To address this issue, we performed Western blot analysis of cytosol Cyt C levels. Interestingly, we found that DOX significantly increased Cyt C protein releasing into the cytosol of myocardial tissue, which was rescued by CYP2J2 treatment (Fig. S2B). These results suggested CYP2J2 overexpression mitigated mitochondrial dysfunction in DOX-treated mice.

To determine the effects of CYP2J2 treatment on myocardial apoptosis, Bcl-2, Bax, cleaved caspase-3, and caspase-3 protein expression levels in heart tissues were determined by western blotting. CYP2J2 overexpression significantly countered the reduction in Bcl-2 levels and the increase in Bax levels in the cardiac tissues of DOX-treated mice. Compared to control mice, a significant increase in the level of cleaved caspase-3 protein was observed in mice treated with DOX, whereas a significant decrease was observed in mice treated with CYP2J2 (Fig. 3D). These results indicate that CYP2J2 protects heart cells against oxidative damage, mitochondrial dysfunction, and apoptosis caused by DOX.

3.4. 14,15-EET suppressed oxidative stress, mitochondrial dysfunction and apoptosis in DOX-exposed H9C2 cells

To investigate the antioxidant effects of 14,15-EET *in vitro*, DHE fluorescence was used to detect ROS levels in H9C2 cells. In H9C2 cells cultured with DOX for 24 h, ROS generation was increased compared to that in control cells, whereas treatment with 14,15-EET

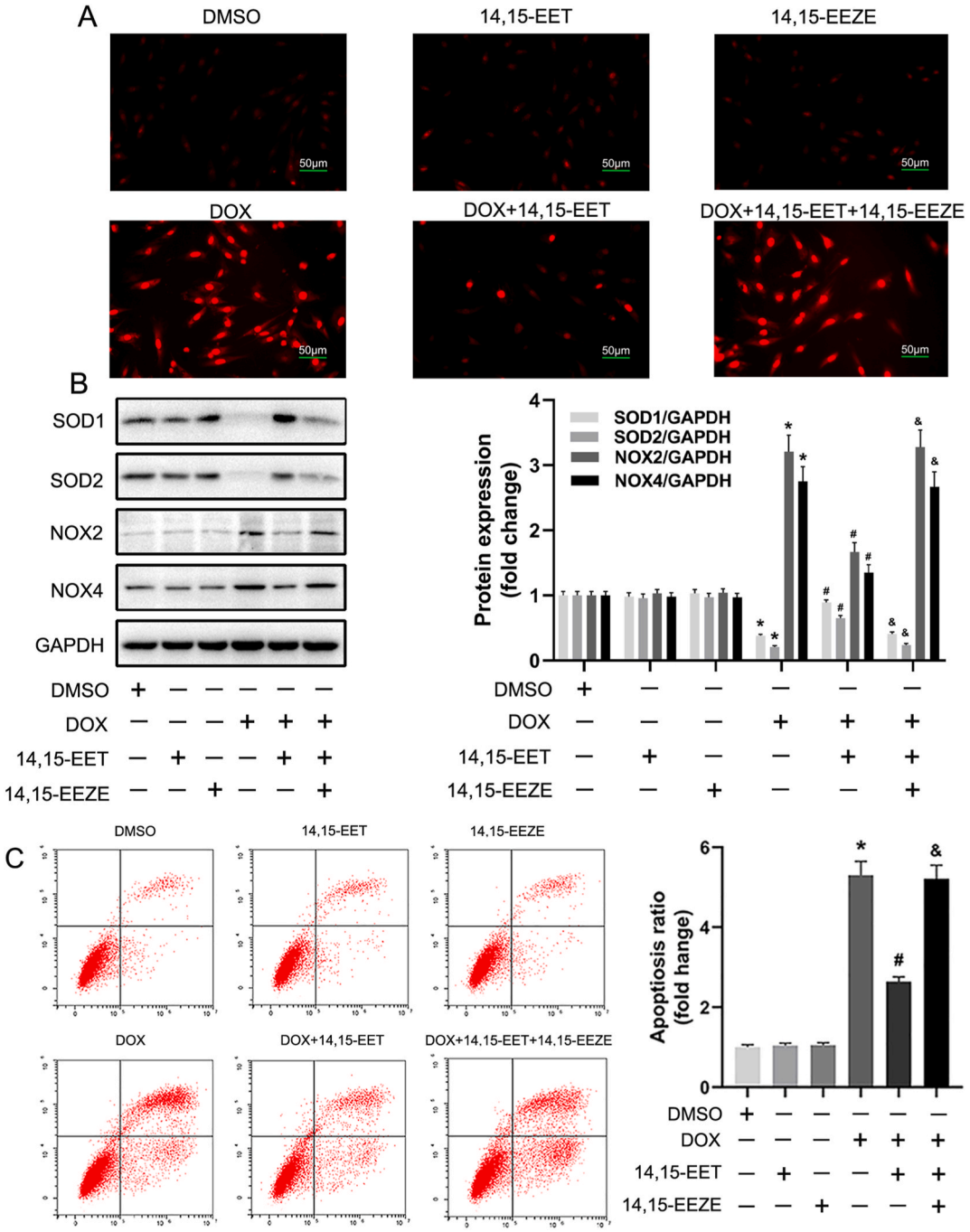

Fig. 4. 14,15-EET suppressed oxidative stress, mitochondrial dysfunction, and apoptosis in DOX-exposed H9C2 cells. (A) DHE staining of H9C2 cells. (B) Representative immunoblots and quantitative analysis of SOD1, SOD2, NOX2, and NOX4 levels in H9c2 cells. (C) H9C2 cells apoptosis were detected via flow cytometry by use of Annexin V/PI staining. (D) Representative immunoblots and quantitative analysis of Bcl-2, Bax, C-caspase-3, and Caspase-3 expression in H9C2 cells. (E) Representative immunoblots and quantitative analysis of *p*-AMPKα, AMPKα, PGC-1α, and UCP2 levels in H9C2 cells. Data are presented as mean ± SEM (n = 3 per group). $^{*}P < 0.05$ vs. DMSO; $^{\#}P < 0.05$ vs. DOX; $^{\&}P < 0.05$ vs. DOX+14,15-EET.

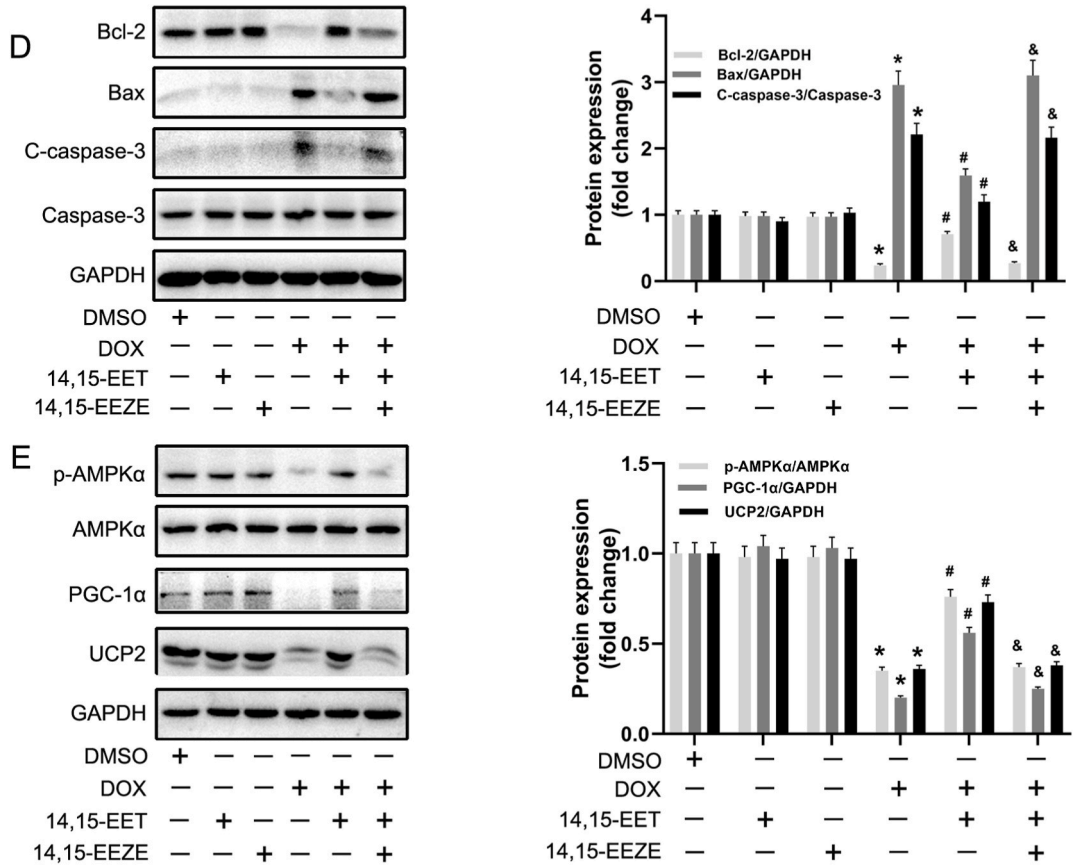

Fig. 4. (*continued*).

significantly reduced DOX-triggered elevations in intracellular ROS levels. Conversely, treatment with the putative EET receptor antagonist 14,15-EEZE abrogated the effect of 14,15-EET on ROS production (Fig. 4A, S4B). Further detection with DCFH-DA staining revealed that 14,15-EEZE reversed the protective effect of 14,15-EET on DOX-induced oxidative stress (Figs. S5A and B). Furthermore, the DOX +14,15-EET group showed significant upregulation of the antioxidative indicators SOD1 and SOD2 and downregulation of the oxidative indicators NOX2 and NOX4 compared to the DOX group (Fig. 4B). The DOX +14,15-EET +14,15-EEZE group showed no significant improvement. The higher the JC-1 monomers (green), the lower the mitochondrial membrane potential. DOX treatment significantly increased the green fluorescence intensity of JC-1 monomers, However, 14,15-EET treatment decreased the intensity of green fluorescence intensity of JC-1 monomers (Figs. S6A and B).

Flow cytometry analysis confirmed a significant reduction in DOX-induced cardiomyocyte apoptosis after 14,15-EET treatment compared with DOX-only treatment, which was abolished by 14,15-EEZE (Fig. 4C). We evaluated the effects of 14,15-EET on the expression of apoptosis-related genes in H9C2 cells. After DOX treatment, western blotting showed a significant increase in Bcl-2 levels following the administration of 14,15-EET, along with a decrease in Bax and cleaved caspase-3 expression. However, the EET receptor antagonist, 14, 15-EEZE, counteracted these effects (Fig. 4D). In line with *in vivo* findings, 14,15-EET treatment significantly increased *p*-AMPK, PGC-1α, and UCP2 protein levels in DOX-treated H9C2 cells, which were partly abolished by 14,15-EEZE application (Fig. 4E). In summary, these results demonstrate that 14,15-EET mitigates DOX-induced oxidative damage, mitochondrial dysfunction, and apoptosis in H9C2 cells.

3.5. AMPK was responsible for EETs-mediated protective roles on DOX-induced cardiotoxicity

To confirm whether AMPK mediates the protective effect of 14,15-EET against DOX-induced cardiomyocyte damage, AMPKα was knocked down by specific siRNA in H9C2 cells. AMPKα protein levels were significantly reduced after transfection AMPKα siRNA (Fig. S3). Subsequently, we explored the roles of AMPKα siRNA in DOX-induced oxidative damage, mitochondrial dysfunction, and apoptosis. As shown in Fig. 5A, S4C, 14,15-EET treatment decreased DOX-induced ROS production. However, these effects were attenuated in the AMPKα siRNA-treated cardiomyocytes. DCFH-DA staining was further demonstrated AMPKα siRNA counteracted the protective effects of 14,15-EET (Figs. S5C and D). Western blotting indicated that AMPKα siRNA partly blocked the 14,15-EET-induced upregulation of SOD1, SOD2 and downregulation of NOX2, NOX4 at the protein level (Fig. 5B). JC-1 staining also suggests that 14,15-EET is required to protect DOX-induced mitochondrial dysfunction through AMPKα (Figs. S6C and D). Flow cytometry results showed

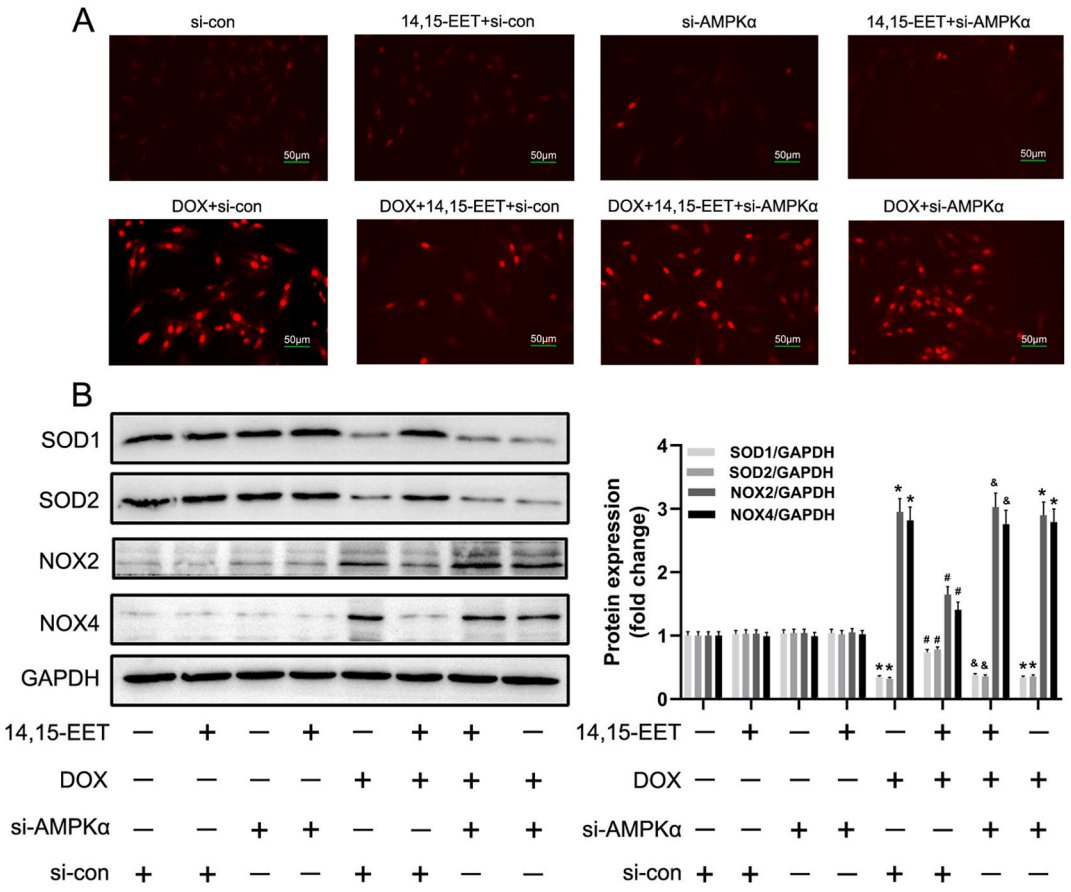

Fig. 5. 14,15-EET decreases oxidative stress, mitochondrial dysfunction and apoptosis in DOX-incubated H9C2 cells through the AMPK pathway. (A) DHE staining of H9C2 cells. (B) Representative immunoblots and quantitative analysis of SOD1, SOD2, NOX2, NOX4 levels in H9C2 cells. (C) H9C2 cell apoptosis was detected via flow cytometry by use of Annexin V/PI staining. (D) Representative immunoblots and quantitative analysis of Bcl-2, Bax, C-caspase-3, and Caspase-3 levels in H9C2 cells. (E) Representative immunoblots and quantitative analysis of PGC-1α, UCP2 expression levels in H9C2 cells. Data are presented as mean ± SEM (n = 3 per group). $^{*}P < 0.05$ vs. si-con; $^{\#}P < 0.05$ vs. DOX + si-con; $^{\&}P < 0.05$ vs. DOX+14,15-EET + si-con.

that AMPKα siRNA prevented the ameliorative effects of 14,15-EET on apoptosis-positive cardiomyocytes (Fig. 5C). In addition, the protective effects of 14,15-EET was partly abolished in AMPKα siRNA-transfected cardiomyocytes, resulting in increased cleaved caspase-3 and Bax protein levels, and reduced Bcl-2 protein levels (Fig. 5D). Similarly, AMPKα siRNA pretreatment inhibited 14,15-EET-mediated upregulation in PGC-1α and UCP2 levels (Fig. 5E). These findings suggest that AMPK is responsible for the protective roles in DOX cardiotoxicity.

4. Discussion

However, the specific mechanism by which anthracyclines cause cardiotoxicity remains unclear. Based on our findings, we conclude that CYP2J2 overexpression counteracts the development of DOX-related toxicity in a mouse model by improving cardiac dysfunction and remodeling, which is linked to diminished oxidative damage and cardiomyocyte apoptosis. Furthermore, exogenous 14,15-EET diminished reactive oxygen species (ROS) production, mitochondrial dysfunction, and apoptosis via the AMPK pathway in H9c2 cells exposed to doxorubicin exposure. Based on these findings, EETs represent a potential approach to reduce chemotherapy-induced cardiotoxicity.

The improvement in systolic function due to an increased ejection fraction and fractional shortening represents an unexpectedly favorable cardiovascular outcome of CYP2J2 overexpression in animals with DOX-induced cardiotoxicity. Cardiac fibrosis is characterized by an aberrant extracellular matrix remodeling and accumulation of collagen fibers in heart, resulting in cardiac dysfunction and congestive heart failure [21,22]. Our results suggested that CYP2J2 can be used as a targeted drug to inhibit cardiac fibrosis. The enzymes LDH, CK-MB, and cTnI, which are located in the cytoplasm of cardiomyocytes, are sensitive indicators of cardiac tissue dysfunction owing to their leakage into serum after cardiomyocyte damage. ANP and BNP, released from the ventricles during

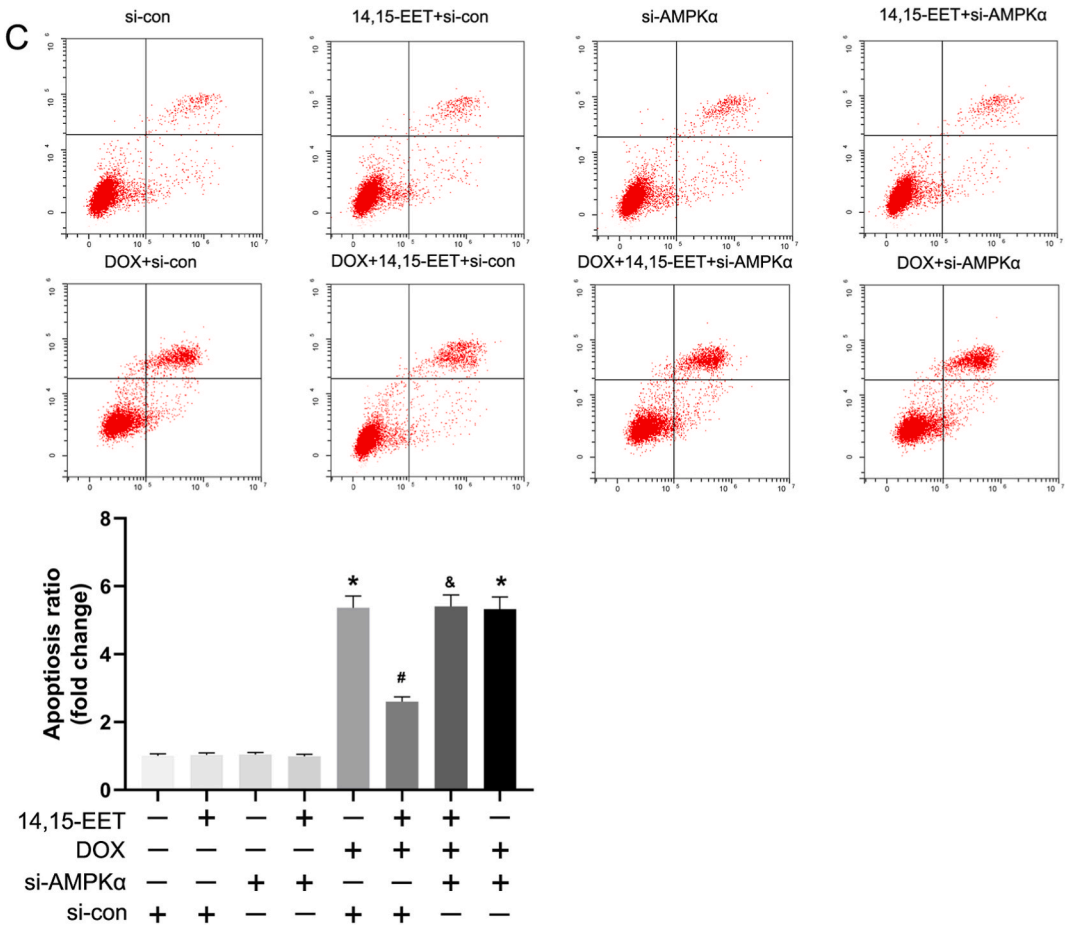

Fig. 5. (*continued*).

stretching are critical markers of cardiomyocyte damage. In other animal models of cardiac damage, overexpression of CYP2J2 has been found to exert similar cardioprotective effects [14]. Here, we measured the levels of these cardiac injury markers and found that the overexpression of CYP2J2 protected against cardiac injury and dysfunction, which may be a potential target for new drugs.

Previous studies have shown that oxidative stress, with excessive ROS production, is the primary cause of DOX-induced cardiotoxicity. After DOX treatment, an imbalance between antioxidants and ROS promotes oxidative stress followed by lipid membrane peroxidation, mitochondrial damage, and apoptosis [23]. The stable end product of lipid peroxidation, MDA, directly indicates the severity of oxidative damage [24]. NOX2 and NOX4 are the two major isoforms of NOXs in the heart and are among the most important sources of cardiac ROS. Depletion of GSH indicates its overutilization in the cellular microenvironment with a redox imbalance, which further promotes oxidative stress and apoptosis [25]. SOD is an antioxidant enzyme that catalyzes the dismutation of superoxide and converts harmful superoxide radicals into hydrogen peroxide [26]. Our results demonstrated that the decreased GSH content and SOD activity, and increased MDA, NOX2, and NOX4 levels after DOX treatment were markedly reversed by CYP2J2 or 14,15-EET, indicating that EETs play cardioprotective roles against oxidative damage and mitochondrial dysfunction during DOX cardiotoxicity.

Substantial evidence has shown that cardiomyocyte apoptosis and subsequent cell loss in DOX-related cardiotoxicity results in cardiac dysfunction and heart failure. DRP1 expression levels are associated with mitochondrial fission-associated GTPase and classical proteins that affect mitochondrial morphological changes, and increased DRP1 expression can promote mitochondrial fission [27]. During doxorubicin metabolism, ROS accumulation in the heart results in cytochrome C release, which leads to caspase-3 activation and initiation of cardiomyocyte apoptosis [28]. Among apoptotic regulatory genes, the caspase and Bcl-2 families play key roles. Bax and Bcl-2 are antagonistic regulatory genes. Specifically, Bax stimulates cytochrome C release from the mitochondria, forming an apoptosome complex in the cytosol. This complex triggers a caspase cascade causing cardiomyocyte apoptosis [29]. Conversely, Bcl-2 can prevent cytochrome C release from the mitochondria and maintain mitochondrial structure and function to inhibit apoptosis [29,30]. In viable cells, caspase-3 is an inactive procaspase and its activation is initiated after a certain subunit is proteolytically cleaved. Subsequently, downstream substrates are cleaved, leading to apoptosis [31]. In the present study, DOX treatment significantly elevated c-caspase-3, Bax, DRP1, and cytosol cytochrome C levels, decreased Bcl-2 expression, and increased the number of apoptotic cells in the heart. However, these effects were ameliorated upon treatment with either CYP2J2 or 14, 15-EET. Consistent with our results, the anti-apoptotic effects of CYP2J2 and EETs were observed in other heart failure models. These findings

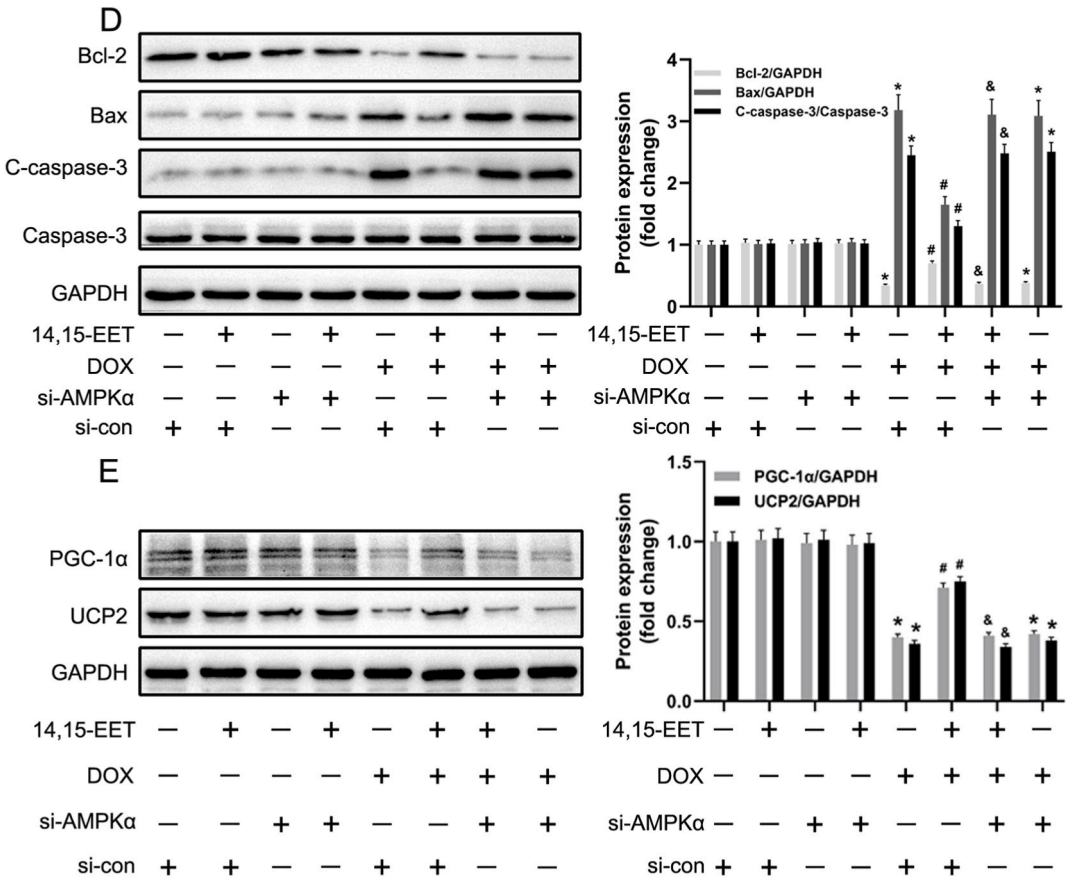

Fig. 5. (*continued*).

indicate that CYP2J2-derived EETs differentially modulate Bcl-2 family expression levels and, in turn, reduce DOX-induced cardiac apoptosis caused by doxorubicin.

AMPK consists of a catalytic α-subunit and two regulatory (β and γ) subunits [12]. Phosphorylation at the THR172 site of the α subunit which serves as the catalytic unit of AMPK, is key to AMPK activation [32], and the β subunit uses its c-terminal domain to bind the α and γ subunits together; the γ subunit is responsible for the allosteric activation of AMPK by AMP [33]. AMPK regulates the ROS/redox equilibrium, endoplasmic reticulum stress, apoptosis, cell proliferation and mitochondrial function to preserve cellular homeostasis. Animals deficient in AMPK exhibit increased cardiac hypertrophy, oxidative stress and energy stress, thereby promoting mitochondrial dysfunction, apoptosis, increased infarct size, and accelerated heart failure [34]. PGC-1α, a critical downstream effector of AMPK, is largely associated with the maintenance and repair of hypoxic and ischemic cardiomyocytes [35]. The AMPK pathway has been shown to exert beneficial effects in the context of DOX cardiotoxicity [13,36]. Lack of AMPK activity leads to mitochondrial ROS perception and decomposition, which resists stress and maintains cellular metabolic balance [37]. Studies have also shown that myocardial AMPK and PGC-1α activation is significantly inhibited in the cardiomyocytes exposure to doxorubicin. As shown in mouse cardiac tissues and H9C2 cells, AMPK activation by overexpression of CYP2J2 or 14,15-EET treatment upregulated PGC1α and UCP2 expression levels after DOX exposure. Conversely, knockdown of AMPK by siRNA inhibited the 14,15-EET-induced PGC1α and UCP2 upregulation and its downstream effects, including antioxidant activities, along with anti-apoptotic activities in DOX-treated H9C2 cells. These results indicate that CYP2J2-derived EETs confer myocardial protection via the AMPK pathway by suppressing oxidative damage, mitochondrial dysfunction, and apoptosis in cardiomyocytes exposed to doxorubicin. Currently, we mainly focused on the fact that CYP2J2 overexpression prevents DOX cardiotoxicity. The lack of results from CYP2J2 knock-out mice is one of the limitations of the present study.

5. Conclusion

Concludingly, we demonstrated that CYP2J2-derived EETs protected against cardiac dysfunction and decreased the oxidative stress, mitochondrial dysfunction, and apoptosis observed in DOX-induced cardiotoxicity. *In vitro* investigations showed that this occurred through the upregulation of the AMPK signaling pathway. These results highlight a novel protective role of EETs against oxidative stress, mitochondrial dysfunction, and apoptosis resulting from chemotherapy-related cardiotoxicity. Thus, EETs may serve

as drug targets to protect against cancer treatment–related cardiotoxicity in clinical settings. The development of EET analogs is evolving as an important research direction for reducing DOX-related cardiotoxicity.

Data availability

All data is contained within the article.

Funding statement

This work was supported by grants from the Natural Science Foundation of Hubei Province, China (2022CFB198) and Tongji Hospital Returns from Studying Abroad Startup Foundation, China (2022hgry008 and 2022hgry023).

Ethics statement

All experimental protocols were conducted in accordance with the Care and Use of Laboratory Animals guidelines set forth by the Institutional Animal Research Committee (NO:TJH-20201006) of Tongji Hospital, Tongji Medical College, Huazhong University of Science and Technology (Wuhan, China).

CRediT authorship contribution statement

Chuanmeng Zhu: Writing - review & editing, Writing - original draft, Formal analysis, Data curation, Conceptualization. **Yang Bai:** Software, Methodology. **Jie Qiu:** Software, Methodology. **Guangzhi Chen:** Writing - review & editing, Resources, Data curation, Conceptualization. **Xiaomei Guo:** Supervision, Project administration, Funding acquisition. **Renfan Xu:** Supervision, Resources, Project administration, Funding acquisition, Conceptualization.

Declaration of competing interest

The authors declare that they have no known competing financial interests or personal relationships that could have appeared to influence the work reported in this paper.

Acknowledgements

We thank the researchers for their suggestions, support, and assistance in preparing this draft.

Abbreviations

AMPK Adenosine monophosphate-activated protein kinase
Bax Bcl-2-associated X protein
Bcl-2 B-cell lymphoma-2
CK-MB creatine kinase MB isoenzyme
cleaved caspase-3 C-caspase-3
cTnT cardiac troponin T
CYP2J2 cytochrome P450 epoxygenase 2J2
DHE Dihydroethidium
DOX doxorubicin
EETs epoxyeicosatrienoic acids
EEZE epoxyeicosa-5(Z)-enoic acid
heart weight/tibial length HW/TL;
LDH lactate dehydrogenase
MDA malondialdehyde
NOX2 nicotinamide adenine dinucleotide phosphate oxidase 2
NOX4 nicotinamide adenine dinucleotide phosphate oxidase 4
PGC-1α peroxisome proliferator-activated receptor gamma coactivator 1-alpha
rAAV-GFP recombinant adeno-associated virus expressing green fluorescent protein
ROS reactive oxygen species
SDS sodium dodecyl sulfate-polyacrylamide;
SOD1 superoxide dismutase 1
SOD2 superoxide dismutase 2
UCP2 uncoupling protein 2

Appendix A. Supplementary data

Supplementary data to this article can be found online at https://doi.org/10.1016/j.heliyon.2023.e23526.

References

[1] K. Renu, V. Ga, P. Bt, S. Arunachalam, Molecular mechanism of doxorubicin-induced cardiomyopathy - an update, Eur. J. Pharmacol. 818 (2018) 241–253.
[2] M. Songbo, H. Lang, C. Xinyong, X. Bin, Z. Ping, S. Liang, Oxidative stress injury in doxorubicin-induced cardiotoxicity, Toxicol. Lett. 307 (2019) 41–48.
[3] Y. Jiang, Y. Jiang, M. Li, Q. Yu, Will nanomedicine become a good solution for the cardiotoxicity of chemotherapy drugs? Front. Pharmacol. 14 (2023), 1143361.
[4] K.B. Wallace, V.A. Sardão, P.J. Oliveira, Mitochondrial determinants of doxorubicin-induced cardiomyopathy, Circ. Res. 126 (7) (2020) 926–941.
[5] C.G. Nebigil, L. Désaubry, Updates in anthracycline-mediated cardiotoxicity, Front. Pharmacol. 9 (2018) 1262.
[6] J.C. Zhou, C.C. Jin, X.L. Wei, R.B. Xu, R.Y. Wang, Z.M. Zhang, et al., Mesaconine alleviates doxorubicin-triggered cardiotoxicity and heart failure by activating PINK1-dependent cardiac mitophagy, Front. Pharmacol. 14 (2023), 1118017.
[7] C.G. Nebigil, L. Desaubry, Updates in anthracycline-mediated cardiotoxicity, Front. Pharmacol. 9 (2018) 1262.
[8] S.A. Al-Kenany, N.N. Al-Shawi, Protective effect of cafestol against doxorubicin-induced cardiotoxicity in rats by activating the Nrf2 pathway, Front. Pharmacol. 14 (2023), 1206782.
[9] T. Monteiro-Alfredo, J.M. Dos Santos, K.A. Antunes, J. Cunha, D. da Silva Baldivia, A.S. Pires, et al., Acrocomia aculeata associated with doxorubicin: cardioprotection and anticancer activity, Front. Pharmacol. 14 (2023), 1223933.
[10] T. Aliwarga, E.A. Evangelista, N. Sotoodehnia, R.N. Lemaitre, R.A. Totah, Regulation of CYP2J2 and EET levels in cardiac disease and diabetes, Int. J. Mol. Sci. 19 (7) (2018) 1916.
[11] Z. He, X. Zhang, C. Chen, Z. Wen, S.L. Hoopes, D.C. Zeldin, et al., Cardiomyocyte-specific expression of CYP2J2 prevents development of cardiac remodelling induced by angiotensin II, Cardiovasc. Res. 105 (3) (2015) 304–317.
[12] S. Herzig, R.J. Shaw, AMPK: guardian of metabolism and mitochondrial homeostasis, Nat. Rev. Mol. Cell Biol. 19 (2) (2018) 121–135.
[13] M. Singh, A.T. Nicol, J. DelPozzo, J. Wei, M. Singh, T. Nguyen, et al., Demystifying the relationship between metformin, AMPK, and doxorubicin cardiotoxicity, Front Cardiovasc Med 9 (2022), 839644.
[14] B. Wang, H. Zeng, Z. Wen, C. Chen, D.W. Wang, CYP2J2 and its metabolites (epoxyeicosatrienoic acids) attenuate cardiac hypertrophy by activating AMPKalpha2 and enhancing nuclear translocation of Akt1, Aging Cell 15 (5) (2016) 940–952.
[15] Z. Cai, G. Zhao, J. Yan, W. Liu, W. Feng, B. Ma, et al., CYP2J2 overexpression increases EETs and protects against angiotensin II-induced abdominal aortic aneurysm in mice, J. Lipid Res. 54 (5) (2013) 1448–1456.
[16] J.G. Jiang, Y.G. Ning, C. Chen, D. Ma, Z.J. Liu, S. Yang, et al., Cytochrome p450 epoxygenase promotes human cancer metastasis, Cancer Res. 67 (14) (2007) 6665–6674.
[17] C. Zhou, J. Huang, Q. Li, C. Zhan, X. Xu, X. Zhang, et al., CYP2J2-derived EETs attenuated ethanol-induced myocardial dysfunction through inducing autophagy and reducing apoptosis, Free Radic. Biol. Med. 117 (2018) 168–179.
[18] Y. Liu, Y. Xu, Y. Yao, Y. Cao, G. Chen, Y. Cai, et al., I-kappaB kinase-epsilon deficiency improves doxorubicin-induced dilated cardiomyopathy by inhibiting the NF-kappaB pathway, Front. Physiol. 13 (2022), 934899.
[19] M. Dai, L. Wu, Z. He, S. Zhang, C. Chen, X. Xu, et al., Epoxyeicosatrienoic acids regulate macrophage polarization and prevent LPS-induced cardiac dysfunction, J. Cell. Physiol. 230 (9) (2015) 2108–2119.
[20] Y.J. Li, P.H. Wang, C. Chen, M.H. Zou, D.W. Wang, Improvement of mechanical heart function by trimetazidine in db/db mice, Acta Pharmacol. Sin. 31 (5) (2010) 560–569.
[21] X. Zhang, C. Hu, N. Zhang, W.Y. Wei, L.L. Li, H.M. Wu, et al., Matrine attenuates pathological cardiac fibrosis via RPS5/p38 in mice, Acta Pharmacol. Sin. 42 (4) (2021) 573–584.
[22] X. Zhang, C. Hu, Y.P. Yuan, P. Song, C.Y. Kong, H.M. Wu, et al., Endothelial ERG alleviates cardiac fibrosis via blocking endothelin-1-dependent paracrine mechanism, Cell Biol. Toxicol. 37 (6) (2021) 873–890.
[23] L. Rochette, C. Guenancia, A. Gudjoncik, O. Hachet, M. Zeller, Y. Cottin, et al., Anthracyclines/trastuzumab: new aspects of cardiotoxicity and molecular mechanisms, Trends Pharmacol. Sci. 36 (6) (2015) 326–348.
[24] D. Tsikas, Assessment of lipid peroxidation by measuring malondialdehyde (MDA) and relatives in biological samples: analytical and biological challenges, Anal. Biochem. 524 (2017) 13–30.
[25] G. Filomeni, D. De Zio, F. Cecconi, Oxidative stress and autophagy: the clash between damage and metabolic needs, Cell Death Differ. 22 (3) (2015) 377–388.
[26] J. Govender, B. Loos, A.M. Engelbrecht, Melatonin: a protective role against doxorubicin-induced cardiotoxicity, Future Oncol. 11 (14) (2015) 2003–2006.
[27] J.Y. Jin, X.X. Wei, X.L. Zhi, X.H. Wang, D. Meng, Drp1-dependent mitochondrial fission in cardiovascular disease, Acta Pharmacol. Sin. 42 (5) (2021) 655–664.
[28] C.Y. Kong, Z. Guo, P. Song, X. Zhang, Y.P. Yuan, T. Teng, et al., Underlying the mechanisms of doxorubicin-induced acute cardiotoxicity: oxidative stress and cell death, Int. J. Biol. Sci. 18 (2) (2022) 760–770.
[29] T.T. Renault, K.V. Floros, J.E. Chipuk, BAK/BAX activation and cytochrome c release assays using isolated mitochondria, Methods 61 (2) (2013) 146–155.
[30] T. Moldoveanu, P.E. Czabotar, B.A.K. Bax, Bok, A coming of age for the BCL-2 family effector proteins, Cold Spring Harbor Perspect. Biol. 12 (4) (2020) a036319.
[31] F. Li, A. Wei, L. Bu, L. Long, W. Chen, C. Wang, et al., Procaspase-3-activating compound 1 stabilizes hypoxia-inducible factor 1alpha and induces DNA damage by sequestering ferrous iron, Cell Death Dis. 9 (10) (2018) 1025.
[32] R. Sahu, T.K. Dua, S. Das, V. De Feo, S. Dewanjee, Wheat phenolics suppress doxorubicin-induced cardiotoxicity via inhibition of oxidative stress, MAP kinase activation, NF-kappaB pathway, PI3K/Akt/mTOR impairment, and cardiac apoptosis, Food Chem. Toxicol. 125 (2019) 503–519.
[33] Q. Afinanisa, M.K. Cho, H.A. Seong, AMPK localization: a key to differential energy regulation, Int. J. Mol. Sci. 22 (20) (2021), 10921.
[34] G. Noppe, C. Dufeys, P. Buchlin, N. Marquet, D. Castanares-Zapatero, M. Balteau, et al., Reduced scar maturation and contractility lead to exaggerated left ventricular dilation after myocardial infarction in mice lacking AMPKalpha1, J. Mol. Cell. Cardiol. 74 (2014) 32–43.
[35] S. Spinelli, G. Begani, L. Guida, M. Magnone, D. Galante, C. D'Arrigo, et al., LANCL1 binds abscisic acid and stimulates glucose transport and mitochondrial respiration in muscle cells via the AMPK/PGC-1alpha/Sirt1 pathway, Mol. Metabol. 53 (2021), 101263.
[36] M. Iwabu, T. Yamauchi, M. Okada-Iwabu, K. Sato, T. Nakagawa, M. Funata, et al., Adiponectin and AdipoR1 regulate PGC-1alpha and mitochondria by Ca(2+) and AMPK/SIRT1, Nature 464 (7293) (2010) 1313–1319.
[37] R.C. Rabinovitch, B. Samborska, B. Faubert, E.H. Ma, S.P. Gravel, S. Andrzejewski, et al., AMPK maintains cellular metabolic homeostasis through regulation of mitochondrial reactive oxygen species, Cell Rep. 21 (1) (2017) 1–9.